

# Random Matrices and Random Permutations

Andrei Okounkov

## Abstract

We prove a version of the conjecture of Baik, Deift, and Johansson which says that with respect to the Plancherel measure on the set of partitions  $\lambda$  of  $n$ , the rows  $\lambda_1, \lambda_2, \lambda_3, \dots$  of  $\lambda$  behave, suitably scaled, like the 1st, 2nd, 3rd, and so on eigenvalues of a Gaussian random Hermitian matrix as  $n \rightarrow \infty$ . Our proof is based on an interplay between maps on surfaces and ramified coverings of the sphere. The subject turns out to have a strong connection to Kontsevich's work on Witten conjectures.

## 1 Introduction

### 1.1

The set  $G^\wedge$  of equivalence classes of irreducible representations  $\pi$  of any finite group  $G$  carries a natural measure which gives a representation  $\pi$  mass  $(\dim \pi)^2/|G|$ . This is a probability measure called the *Plancherel* measure because the Fourier transform

$$L^2(G, \mu_{\text{Haar}})^G \xrightarrow{\text{Fourier}} L^2(G^\wedge, \mu_{\text{Plancherel}})$$

is an isometry just like in the classical Plancherel theorem.

Logan and Shepp [31] and, independently, Vershik and Kerov [37] (see also the paper [38] which contains complete proofs of the results announced in [37]) discovered the following measure concentration phenomenon for the Plancherel measures of the symmetric groups  $S(n)$  as  $n \rightarrow \infty$ . The set  $S(n)^\wedge$  is labeled by partitions of  $n$  or, equivalently, by Young diagrams with  $n$  squares. Take such a diagram, scale it in both directions by a factor of  $n^{-1/2}$  so that to obtain a shape of unit area, and rotate  $135^\circ$  like in Figure 1.

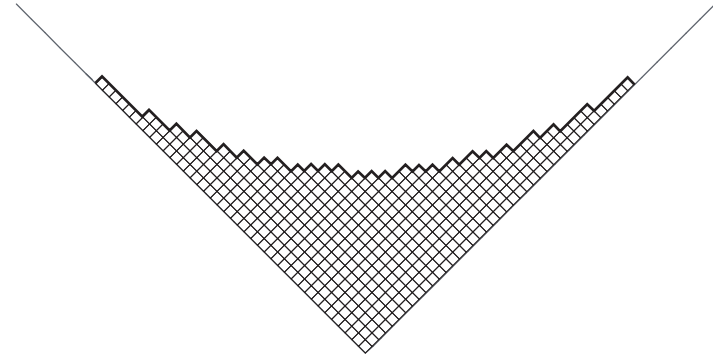


Figure 1: A Young diagram rotated  $135^\circ$

The boundary of this shape is a polygonal line which is thickened in Figure 1. In this way the Plancherel measure becomes a measure on the space of continuous functions. It was shown in [31, 37, 38] that as  $n \rightarrow \infty$ , this measure converges to the delta measure at the following function

$$\Omega(x) = \begin{cases} \frac{2}{\pi} (x \arcsin(x/2) + \sqrt{4 - x^2}) & |x| \leq 2, \\ |x| & |x| \geq 2, \end{cases} \quad (1.1)$$

whose graph is drawn in Figure 2.

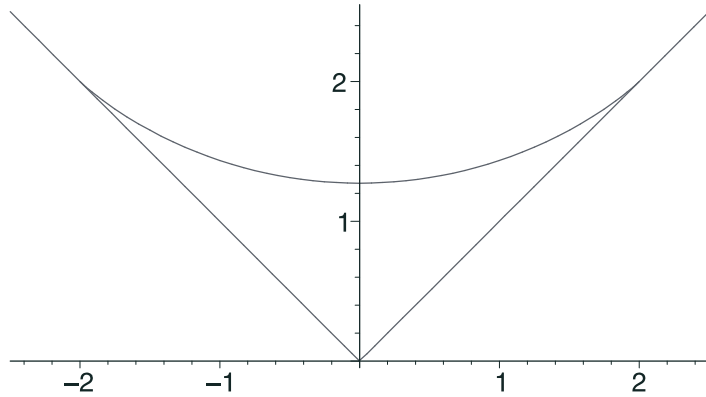


Figure 2: The limit curve  $\Omega(x)$

The constant 2 in (1.1) means that the first part of  $\lambda$  should behave like  $\sim 2\sqrt{n}$  as  $n \rightarrow \infty$ . Indeed, it was shown in [37, 38] that  $\lambda_1/\sqrt{n} \rightarrow 2$  in probability (in [31] the inequality  $\lim \lambda_1/\sqrt{n} \geq 2$  was obtained). This

constant 2 corresponds to the constant 2 in the Ulam problem about the length of the longest increasing subsequence in a random permutation; it was also obtained by different means in [1, 15, 33]. About the history of the Ulam problem see [2] and vast literature cited there.

The next term in the asymptotic of the Plancherel measure was computed by Kerov in [19] who showed that the Plancherel measure behaves like

$$\Omega(x) + \frac{U(x)}{n^{1/2}} + o\left(\frac{1}{n^{1/2}}\right), n \rightarrow \infty, \quad (1.2)$$

where  $U(x)$  is the following Gaussian random process

$$U(x) = \sum_{k=1}^{\infty} \zeta_k \frac{U_k(x)}{\sqrt{k+1}}.$$

Here  $U_k(x)$  are the Tchebychef polynomials of the second kind

$$U_k(2 \cos \phi) = \frac{\sin(k+1)\phi}{\sin \phi}$$

and  $\zeta_k$  are independent standard normal variables. Observe that near the endpoints  $x = \pm 2$  the formula (1.2) becomes inadequate because the series diverges at the endpoints.

## 1.2

The behavior of the Plancherel measure near the edges of  $[-2, 2]$  has been the subject of intense recent studies and numerical experiments, see [2] and references therein. It has been conjectured that this behavior, suitably scaled, is identical to the behavior of the eigenvalues of a random Hermitian matrix near the edge of the Wigner semicircle. More precisely, consider a random  $n \times n$  matrix

$$H = \begin{pmatrix} & \vdots & \\ \dots & h_{ij} & \dots \\ & \vdots & \end{pmatrix}_{1 \leq i, j \leq n}, \quad h_{ij} = \overline{h_{ji}}$$

such that the real and imaginary parts

$$h_{ij} = u_{ij} + iv_{ij}$$

are independent normal variables with mean 0 and variance 1/2. Let

$$E_1 \geq E_2 \geq E_3 \geq \dots$$

be the eigenvalues of  $H$ . Introduce the variables  $y_i$

$$y_i = n^{2/3} \left( \frac{E_i}{2n^{1/2}} - 1 \right), \quad i = 1, 2, \dots \quad (1.3)$$

Then as  $n \rightarrow \infty$  the  $y_i$ 's have a limit distribution which was studied in [12, 36] and other papers. In particular, the correlation functions of this random point process are certain determinants built from Airy functions. The distributions of individual  $y_i$ 's were obtained by Tracy and Widom in [36]; they involve certain solutions of the Painlevé II equation.

Similarly, let  $\lambda = (\lambda_1, \lambda_2, \dots)$  be a partition and set (note the difference with (1.3) in the exponent of  $n$ )

$$x_i = n^{1/3} \left( \frac{\lambda_i}{2n^{1/2}} - 1 \right), \quad i = 1, 2, \dots \quad (1.4)$$

Baik, Deift, and Johansson conjectured that the limit distribution of the  $x_i$ 's exists and coincides with that of the  $y_i$ 's. They verified this conjecture for the distribution of  $x_1$  and  $x_2$  in [2] and [3], respectively, using very advanced analytic methods.

### 1.3

In this paper we give a combinatorial proof of the following result. Consider the points  $x_1, x_2, \dots$  as a random measure on  $\mathbb{R}$  with masses 1 placed at the points  $x_i$ ,  $i = 1, 2, \dots$ . Consider its Laplace transform

$$\widehat{x}(\xi) = \sum_{i=1}^{\infty} \exp(\xi x_i), \quad \xi > 0,$$

this is a random process on  $\mathbb{R}_{>0}$ . Define  $\widehat{y}(\xi)$  similarly. We shall denote expectation by angle brackets.

**Theorem 1** *In the  $n \rightarrow \infty$  limit, all mixed moments of the random variables  $\widehat{x}(\xi)$  exist and are identical to those of  $\widehat{y}(\xi)$ , that is,*

$$\left\langle \widehat{x}(\xi_1) \cdots \widehat{x}(\xi_s) \right\rangle = \left\langle \widehat{y}(\xi_1) \cdots \widehat{y}(\xi_s) \right\rangle, \quad (1.5)$$

for any  $s = 1, 2, \dots$  and any numbers  $\xi_1, \dots, \xi_s > 0$ .

Our proof utilizes the equivalence of two points of view on topological surfaces (or algebraic curves). One way to think about a surface is to imagine it glued from polygons by identifying sides of polygons in pairs. Such a representation is a combinatorial structure called a *map* on a surface. In connection with quantum gravity, it has been long known that maps are most intimately related to random matrices, see e. g. [39] for an elementary introduction.

Another equally classical way of representing a surface is to realize it as a ramified covering of a simpler surface such as the sphere  $S^2$ . It is classically known that every problem about the combinatorics of covering has a translation into a problem about permutations (which arise as monodromies around the ramification points).

The two sides in (1.5) have a combinatorial interpretation as asymptotics of certain maps and coverings, respectively. We produce a correspondence between the two enumeration problems and show that its deviation from being a bijection is negligible in the  $n \rightarrow \infty$  limit. This can be also interpreted as saying that two random ways of producing a surface yield the same distribution of topologies in the  $n \rightarrow \infty$  limit.

## 1.4

There exists a general analytic machinery, see [35], which allows to pass from the convergence of Laplace transforms like in Theorem 1 to the convergence of the distributions of the individual  $x_i$ 's. In the present paper, however, we would like to concentrate on the combinatorial side of the problem.

An analytic proof of the Baik–Deift–Johansson conjecture was found subsequently in [8] and, independently, in [16]. This approach is based on an exact formula for the so-called correlation functions of the poissonized Plancherel measure and the depoissonization machinery, much in the spirit of [15, 2, 3]. This exact formula for correlation functions is a special case of the result obtained in [7]. Later, the results of [7] were considerably generalized in [29].

Same approach allows to understand the fine asymptotics of the Plancherel measures not only on “the edge of the spectrum”, as in Theorem 1, but also “in the bulk”. This was done in [8].

## 1.5

The existence of a connection between Plancherel measures and random matrices has been actively advocated by S. Kerov (both in a series of papers, see e.g. [20, 21, 22], and, especially, in private conversations). The simplest evidence of such a connection is the fact that the so called *transition distribution* for the limit shape  $\Omega$  coincides with the Wigner semicircle. Random matrices also enter the representation theory of symmetric groups via the free probability theory. For a detailed discussion of the interplay between symmetric groups and free probability see the paper [5] by P. Biane. Our results explain, at least to some extend, this connection.

Recall that by a formula due to Burnside [25] (which was rediscovered by Dijkgraaf and Witten [10]) the enumeration of  $d$ -fold ramified coverings of a sphere with prescribed monodromies may be expressed as a certain average with respect to the Plancherel measure on  $S(d)^\wedge$ . There exists a parallel combinatorial problem of counting covers of a torus which (by Burnside-Dijkgraaf-Witten) is related to the uniform measure on partitions. The corresponding averages were computed in [6]. These averages are Fourier coefficients of certain quasi-modular forms and a suitable generating function for them can be evaluated in terms of determinants built from genus 1 theta functions and their derivatives. Further applications of results of [6] (in particular, to asymptotic problems) are considered in [11].

## 1.6

A curious fact is that the subject exhibits a strong connection to Kontsevich's work on the Witten conjectures [18]. More precisely, the Laplace transforms of map (or covering) enumeration asymptotics (see Propositions 1 and 2) becomes identical to the main formula in [18] (the boxed formula on page 10 of [18]) after the Laplace transform variables in [18] are replaced by their *square roots*. This certainly must have some mathematical and physical explanation.

## 1.7

The reader would be hardly surprised to learn that our main technical tool on the symmetric group side are the Jucys–Murphy elements [17, 26, 9]. In recent years, they have become all-purpose heavy-duty technical tools in representation theory of  $S(n)$ . As a question of method, the whole represen-

tation theory of  $S(n)$  can be derived from some simple properties of these elements [30]. Their use is crucial in the classification of admissible representations of  $S(\infty)$ , see [27], in many asymptotic problems related to  $S(\infty)$  [5, 24], higher Capelli identities [28] etc. The observation that in the  $n \rightarrow \infty$  the spectral measures (in the regular representation) of these elements becomes the Wigner semicircle was made by P. Biane in [4].

The Jucys–Murphy elements generate a Gelfand-Zetlin type maximal commutative subalgebra in the group algebra of  $S(n)$ . Therefore, all asymptotic problems related to branching, such as character values at fixed cycle types are encoded in their spectra.

## 1.8

The author would like to thank A. Eskin for discussions related to the subject of the article and NSF for financial support under grant DMS–9801466.

# 2 Random Matrices

## 2.1

The relation between maps on surfaces and random matrices via the Wick formula is well known. Classical examples of exploiting this relation are, for example, the papers [14, 18]. A very accessible introduction can be found, for example, in [39]. See also, for example, [13] for a physical survey.

Nonetheless, we recall some well-known things in order to facilitate the comparison with the enumeration of coverings.

Consider a random Hermitian matrix

$$H = \begin{pmatrix} & \vdots & \\ \dots & h_{ij} & \dots \\ & \vdots & \end{pmatrix}_{1 \leq i, j \leq n}, \quad h_{ij} = \overline{h_{ji}}$$

such that the real and imaginary parts

$$h_{ij} = u_{ij} + iv_{ij}$$

are independent normal variables with mean 0 and variance  $1/2$ . We shall

be interested in the asymptotics of

$$\frac{1}{2^{|k|} n^{|k|/2}} \left\langle \prod_{j=1}^s \text{tr } H^{k_j} \right\rangle, \quad k_i \sim \xi_j n^{2/3} \quad (2.1)$$

as  $n \rightarrow \infty$  and some fixed  $\xi_1, \dots, \xi_s > 0$ . Here  $|k| = \sum_i k_i$ . Similar averages were considered by many authors, see for example [34, 35] and references therein. Since by (1.3)

$$\left( \frac{E_i}{2n^{1/2}} \right)^{\xi_j n^{2/3}} \rightarrow \exp(\xi_j y_i), \quad n \rightarrow \infty,$$

is clear that only the eigenvalues near the edges of the Wigner's semicircle contribute to the asymptotics of (2.1).

By symmetry, it is clear that (2.1) vanishes if  $|k|$  is odd and if  $|k|$  is even then then it is a sum of  $2^{s-1}$  terms coming from various combinations of the maximal and minimal eigenvalues of  $H$ . In the sequel, we shall always assume that  $|k|$  is even. In this case, there are  $2^{s-1}$  possible choices of parity of each individual  $k_i$  and it is easy to see that by taking a suitable linear combination we can single out the contribution

$$\left\langle \hat{y}(\xi_1) \cdots \hat{y}(\xi_s) \right\rangle \quad (2.2)$$

of only maximal eigenvalues.<sup>1</sup> Therefore, instead of working with expectations like (2.2) we can work with expectations (2.1) which is more convenient.

From the Wick formula one obtains

$$\frac{1}{2^{|k|} n^{|k|/2}} \left\langle \prod_{j=1}^s \text{tr } H^{k_j} \right\rangle = \frac{1}{2^{|k|}} \sum_{\mathcal{S}} n^{\chi(\mathcal{S})-s} |\text{Map}_{\mathcal{S}}(k_1, \dots, k_s)|, \quad (2.3)$$

where the sum is over all homeomorphisms types of orientable 2-dimensional topological manifolds  $\mathcal{S}$ , not necessarily connected,  $\chi(\mathcal{S})$  is its Euler number, and  $\text{Map}_{\mathcal{S}}(k_1, \dots, k_s)$  is the set of solutions to the the following combinatorial problem. Take  $s$  polygons: a  $k_1$ -gon, a  $k_2$ -gon, and so on. Fix their orientations and a mark a vertex on each as in Figure 3 (we mark a vertex to distinguish a  $k$ -gon from its  $(k-1)$  rotations). Now consider all possible

---

<sup>1</sup>One can, in fact, easily see that the distribution of maximal and minimal eigenvalues become independent as  $n \rightarrow \infty$ ,

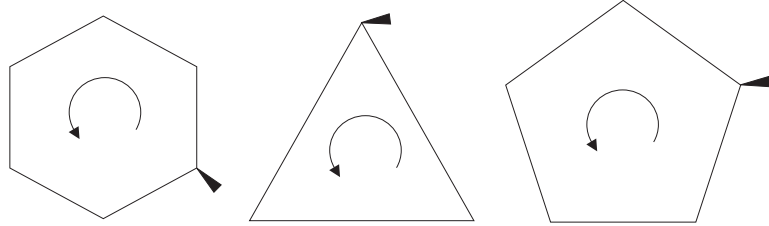


Figure 3: Polygons with orientation and marked vertices

ways to glue their sides in pairs in a way consistent with orientation. The set  $\text{Map}_S$  consists of all glueings which produce a surface homeomorphic to  $S$ .<sup>2</sup>

We are interested in the asymptotics of the numbers  $|\text{Map}_S(k_1, \dots, k_s)|$  as the  $k_i$ 's go to the infinity. Obviously, it is sufficient to consider this asymptotics for connected surfaces  $S$ . From now on, we shall assume that  $S$  is a connected surface of genus  $g$  (that is,  $\chi(S) = 2 - 2g$ ) and write  $\text{Map}_g$  instead of  $\text{Map}_S$ . Also, we assume that  $|k|$  is even because, otherwise, the set of maps is clearly empty.

For a connected surface, we shall see that

$$|\text{Map}_g(t \cdot \xi_1, \dots, t \cdot \xi_s)| \sim \text{const } t^{3g-3+3s/2} 2^{t|\xi|}.$$

We denote by  $\text{map}_g(\xi)$  the constant in the above formula and define  $\text{map}_S$  for a general  $S$  similarly. With this notation, we have (in simplest case when all  $k_i$ 's are even)

$$\frac{1}{2^{|k|} n^{|k|/2}} \left\langle \prod_{j=1}^s \text{tr } H^{k_i} \right\rangle \rightarrow \sum_S \text{map}_S(\xi_1, \dots, \xi_s), \quad k_i \sim \xi_i n^{2/3}. \quad (2.4)$$

Note that the function  $\text{map}_S(\xi_1, \dots, \xi_s)$  is homogeneous of total degree  $\frac{3}{2}(s - \chi(S))$  and also positive for positive values of  $\xi$ . Because of positivity of all terms there are no issues like absolute convergence for series like (2.4).

## 2.2

As the simplest example, consider the case  $g = 0$  and  $s = 1$ , that is, we want to glue a sphere from a  $k$ -gon. One can easily see that one obtains a sphere if

---

<sup>2</sup>Our definition of a map is different from the more common one which does not require the choice of marked vertices. Our present definition is more suitable for our purposes.

and only if lines connecting the identified sides do not intersect (also observe, that the boundary of the polygon becomes a tree in the sphere), see Figure 4.

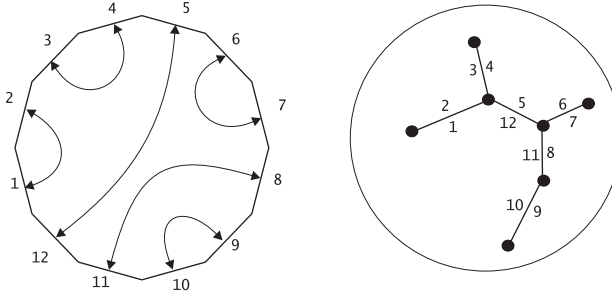


Figure 4: A map on the sphere

The number of such *noncrossing* pairings is the Catalan number

$$|\text{Map}_0(2k)| = \frac{1}{k+1} \binom{2k}{k}$$

from where one obtains

$$\text{map}_0(\xi) = \frac{1}{\sqrt{\pi}} \left( \frac{\xi}{2} \right)^{-3/2}. \quad (2.5)$$

Since  $\deg \text{map}_g(\xi) > 0$  for  $g > 0$ , we have

$$\langle \hat{y}(\xi) \rangle \sim \sqrt{2/\pi} \xi^{-3/2}, \quad \xi \rightarrow +0.$$

This reflects the fact that the density of the  $y_i$ 's is asymptotic to  $\frac{2^{3/2}}{\pi} \sqrt{-y}$  as  $y \rightarrow -\infty$ , see the plots in Figure 5. For future reference, recall the generating function

$$\mathbf{f}(z) = \sum_k z^k |\text{Map}_0(k)| = \frac{1 - \sqrt{1 - 4z^2}}{2z^2}. \quad (2.6)$$

Another special example worth considering is the case  $s = 2, g = 0$ . These are the two cases not covered by the general construction which we are about to explain.

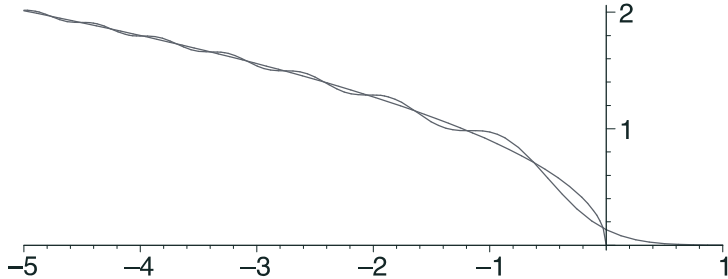


Figure 5: Density of the  $y_i$ 's versus  $2^{3/2}\sqrt{-x}/\pi$

### 2.3

We shall now count the the maps in all cases but  $s = 1, 2$ ,  $g = 0$ . In order to establish connection with random permutations it is not necessary to actually compute the number; it suffices to establish just the general pattern of the combinatorial enumeration which occurs. Nonetheless, we do the computations because the final answer has a striking resemblance to the main formula of [18].

In counting the maps, we shall take the usual combinatorial route and construct a functions from the set of maps onto a simpler set such that the fibers of this functions are easy to understand. Our target set will be the set of pairs  $(\Gamma, \ell)$ , where  $\Gamma \in \Gamma_{g,s}^{\geq 3}$  is a ribbon graphs of genus  $g$ ,  $s$  cells numbered by  $1, 2, \dots, s$ , and vertices of valence  $\geq 3$ ;  $\ell$  is a metric on the boundary  $\partial\Gamma$  of  $\Gamma$ .

Recall that one of many equivalent definition of a *ribbon graph* (or fat-graph) is the following. It is a union of vertices (which are small disks or polygons; we shall paint them grey in the figures) which are connected by ribbons (edges). The boundary  $\partial\Gamma$  of a ribbon graph  $\Gamma$  is an ordinary graph whose edges are the borders of the ribbons. Let  $s$  be the number of connected components of  $\partial\Gamma$ . Filling each component of  $\partial\Gamma$  with a disk produces a closed surface. The genus of  $\Gamma$  is, by definition, the genus of that surface. The components of  $\partial\Gamma$  (or the disks filling them) are called the *cells* of  $\Gamma$ . We shall consider ribbon graphs with  $s$  cells and suppose that the cells are numbered by  $1, 2, \dots, s$ .

Given a map on a surface  $S$ , we consider the the graph on  $S$  formed by vertices and edges of the original polygons. A small neighborhood of this graph is a ribbon graph. The numbering of the cells comes from the numbering of the polygons of the map. For example, consider the map on

the torus which is drawn in Figure 6. The corresponding ribbon graph is

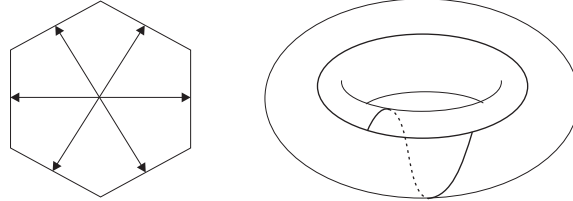


Figure 6: A map on the torus

displayed in Figure 7. There is only one cell in this example.

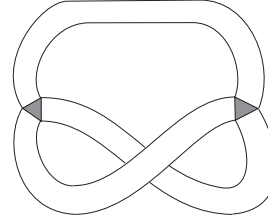


Figure 7: The corresponding ribbon graph

We equip the boundary of this graph with the metric  $\ell$  in which all edges have unit length.

We now wish to eliminate all vertices of valence  $\leq 2$  from our ribbon graph. First, we collapse the univalent vertices as in Figure 8 (the numbers illustrate what we do with the metric  $\ell$ ). After that, the vertices of valence

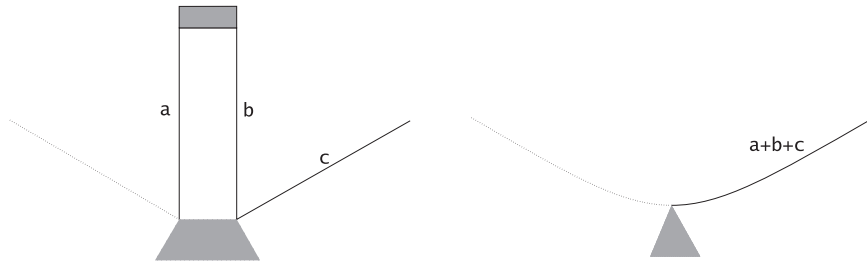


Figure 8: Collapsing of univalent vertices

2 are eliminated as in Figure 9.



Figure 9: Elimination of 2-valent vertices

In the end, we get the following. If we are in two exceptional cases  $g = 0$ ,  $s = 1, 2$  then we get a point and circle, respectively. In all other cases we get a ribbon graph  $\Gamma \in \Gamma_{g,s}^{\geq 3}$ . From the computation of the Euler number it follows that

$$\sum_{v \in v(\Gamma)} (\text{val}(v) - 2) = 4g - 4 + 2s, \quad (2.7)$$

where  $v(\Gamma)$  is the set of vertices of  $\Gamma$ .

We also get a metric  $\ell$  on  $\partial\Gamma$ . An obvious property of this metric is that the lengths of the  $s$  cells  $C_1, \dots, C_s$  of  $\Gamma$  equal  $k_1, k_2, \dots, k_s$

$$\ell(C_i) = k_i, \quad i = 1, \dots, s.$$

All this is, of course, very similar to the stratification of the moduli space of curves of genus  $g$  with  $s$  marked points by means of Strebel differentials, see e. g. [18].

## 2.4

We now want to compute how many maps correspond to a given pair  $(\Gamma, \ell)$ . First, look at a single edge of  $\Gamma$  let  $p$  and  $q$  the lengths of its two boundaries in metric  $\ell$ . We wish to compute how many different configurations produce this data after the elimination of vertices of valence  $\leq 2$ .

This means that we must compute the number of ribbon graphs of the form shown in Figure 10 with the length of the upper boundary and lower boundary being  $p$  and  $q$ , respectively. The trees in Figure 10 stand for (possibly empty) ribbon graphs which disappear after collapsing all univalent vertices. (Thus, those are forests in the usual sense of graph theory and we shall, therefore, call them *forests*).

Remark that a forest is not allowed at one of the ends of both upper and lower boundary. This corresponds to our convention (see Figure 8) on where we put the length of a collapsing edge. However, a simple shift as in Figure

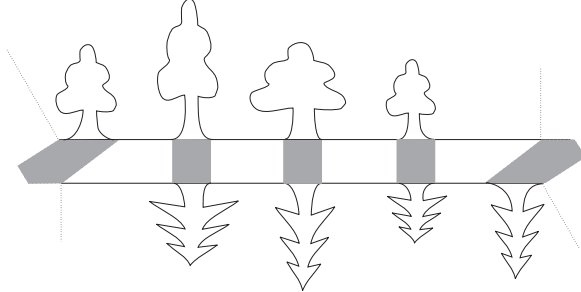


Figure 10: A ribbon graph which collapses to an edge

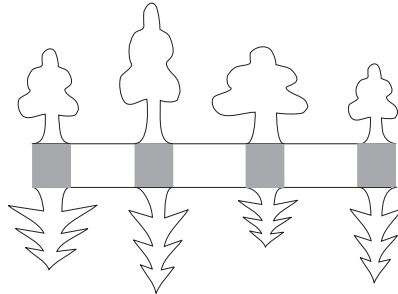


Figure 11: A ribbon graph on the sphere corresponding to the graph in Figure 10

11 which reduces the length of both boundaries by 1, takes care of this small inconvenience. Now it is clear that to obtain a ribbon graph like in Figure 11 one just takes any map from  $\text{Map}_0(p+q-2)$  and calls the first  $(p-1)$  sides the upper boundary, and rest — the lower boundary. Therefore, we get a Catalan number provided  $p+q$  is even (and 0 otherwise). Asymptotically, this means that there are

$$\sim \frac{1}{\sqrt{2\pi}} \frac{2^{p+q}}{(p+q)^{3/2}}, \quad p+q \rightarrow \infty, \quad (2.8)$$

ribbon graphs which collapse to an edge with length of the upper and lower boundary equal to  $p$  and  $q$ , respectively.

Observe that the difference between  $|\text{Map}_0(p+q-2)|$  and  $|\text{Map}_0(p+q)|$  is a factor of  $\sim \frac{1}{2^2}$ . In what follows we shall see much counting of powers of 2. Since keeping track of these powers is important, let us give another explanation of the fact that two missing forests produce a factor of  $\sim \frac{1}{4}$  in the asymptotics.

One can easily write down a generating function enumerating the graphs like in Figure 11

$$f(z_1, z_2) = \sum_{p,q} (\# \text{ of graphs with given } p \text{ and } q) z_1^p z_2^q.$$

One finds out that, just like in case of (2.5) and (2.6), the asymptotics (2.8) is determined by the behavior of this function near the point  $(\frac{1}{2}, \frac{1}{2})$ . Planting (resp. removing) a forest corresponds to multiplication (resp. division) by the generation function  $\mathbf{f}$  defined in (2.6). But  $\mathbf{f}(\frac{1}{2}) = 2$  !

## 2.5

Given a graph  $\Gamma \in \Gamma_{g,s}^{\geq 3}$  and a metric  $\ell$ , let  $\text{Map}_{g,\Gamma,\ell}$  denote the set of all maps which collapse to  $(\Gamma, \ell)$ . Similarly, set  $\text{Map}_{g,\Gamma} = \bigcup_{\ell} \text{Map}_{g,\Gamma,\ell}$ .

The result (2.8) of the previous section implies that

$$|\text{Map}_{g,\Gamma,\ell}| \sim \frac{1}{|\text{Aut}(\Gamma)|} \frac{2^{|k|}}{(2\pi)^{|e(\Gamma)|/2}} \prod_1^s k_i \prod_{e \in e(\Gamma)} (\ell_{1,e} + \ell_{2,e})^{-3/2}. \quad (2.9)$$

Here  $e(\Gamma)$  is the set of edges of  $\Gamma$ ,  $\ell_{1,e}$  and  $\ell_{2,e}$  are the lengths of the two borders of  $e$  in metric  $\ell$ , and  $\text{Aut}(\Gamma)$  is the automorphism group of  $\Gamma$  (by definition, the automorphisms of  $\Gamma$  must preserve cells). The factor  $\prod k_i$  comes from the fact that we can place the marked point of each polygon at an arbitrary point of the corresponding component of  $\partial\Gamma$ . More precisely, to avoid counting the same map several times, we have to account for the automorphisms group of  $\Gamma$  and this is reflected in division by the order  $|\text{Aut}(\Gamma)|$  of this group.

Next we want to perform summation over all metrics  $\ell$ . This means summation over points in  $\mathbb{R}_{\geq 0}^{2|e(\Gamma)|}$  satisfying the following properties

1. the values of  $\ell$  are integers and for any  $e \in e(\Gamma)$  the sum  $\ell_{1,e} + \ell_{2,e}$  is an even integer
2. the perimeters of the  $s$  cells are equal to  $k_1, \dots, k_s$ , respectively

Clearly, the second condition defines a convex polytope (which we shall denote by  $\text{Met}_{\Gamma}(k)$ ) of dimension

$$\dim \text{Met}_{\Gamma}(k) = 2|e(\Gamma)| - s$$

and the first describes a sublattice of index  $|e(\Gamma)|$  in  $\mathbb{Z}^{2|e(\Gamma)|}$ .

The summand in the sum

$$|\text{Map}_{g,\Gamma}| = \sum_{\ell} |\text{Map}_{g,\Gamma,\ell}|$$

is homogeneous of degree  $s - \frac{3}{2}|e(\Gamma)|$ . Therefore, if the  $k_i$ 's go to infinity in such a way that

$$k_i \sim t \cdot \xi_i, \quad t \rightarrow \infty,$$

we obtain

$$\begin{aligned} \text{Map}_{g,\Gamma} \sim & \\ \frac{t^{|e(\Gamma)|/2}}{|\text{Aut}(\Gamma)|} \frac{2^{|k|-3|e(\Gamma)|/2+1}}{\pi^{|e(\Gamma)|/2}} \prod_1^s \xi_i \int_{\text{Met}_{\Gamma}(\xi)} d\ell \prod_{e \in e(\Gamma)} (\ell_{1,e} + \ell_{2,e})^{-3/2}. & (2.10) \end{aligned}$$

Here the normalization of the Lebesgue measure on the polytope  $\text{Met}_{\Gamma}(\xi)$  corresponds to the lattice  $\mathbb{Z}^{2|e(\Gamma)|}$  in the following sense. Consider the linear space associated with the affine span of  $\text{Met}_{\Gamma}(\xi)$ ; this is the same as the linear span of  $\text{Met}_{\Gamma}(0)$ . We normalize the Lebesgue measure on it in such a way that

$$|A \cap t^{-1}\mathbb{Z}^{2|e(\Gamma)|}| \sim t^{2|e(\Gamma)|-s} \int_A d\ell, \quad t \rightarrow \infty$$

for an open set  $A$  in this linear space. Because of the parity conditions on  $\ell$  imposed for every edge  $e \in e(\Gamma)$ , we are actually counting not the points in  $\mathbb{Z}^{2|e(\Gamma)|}$  but rather points in a sublattice of index  $2^{|e(\Gamma)|-1}$  (one of the parity conditions is redundant once the total perimeter is fixed). This is reflected in the fact that the exponent of 2 in (2.9) and (2.10) differ by  $|e(\Gamma)| - 1$ .

Observe, that (2.10) grows like  $t^{|e(\Gamma)|/2}$  as  $t \rightarrow \infty$ . Therefore, the asymptotics of the sum over all  $\Gamma \in \Gamma_{g,s}^{\geq 3}$  is determined by only those  $\Gamma$  which have the maximal number of edges. Equivalently, by invariance of the Euler number, they must have the maximal number of vertices. From (2.7) it follows that this happens if and only if all vertices of  $\Gamma$  are trivalent. Denote by  $\Gamma_{g,s}^3$  the subset of  $\Gamma_{g,s}^{\geq 3}$  formed by trivalent graphs. Remark that every  $\Gamma \in \Gamma_{g,s}^3$  has  $6g - 6 + 3s$  edges.

Therefore, we have established the following result

$$\frac{\text{map}_g(\xi_1, \dots, \xi_s)}{\xi_1 \cdots \xi_s} = \frac{2}{(8\pi)^{3g-3+3s/2}} \sum_{\Gamma \in \Gamma_{g,s}^3} \frac{1}{|\text{Aut}(\Gamma)|} \int_{\text{Met}_\Gamma(\xi)} d\ell \prod_{e \in e(\Gamma)} (\ell_{1,e} + \ell_{2,e})^{-3/2}. \quad (2.11)$$

Using the integral

$$\frac{1}{\sqrt{\pi}} \int_0^\infty \int_0^\infty \frac{e^{-ax-by}}{(x+y)^{3/2}} dx dy = \frac{2}{\sqrt{a} + \sqrt{b}}, \quad \Re a, \Re b > 0.$$

one can compute the Laplace transform of (2.11) in a compact form. Take  $z_1, \dots, z_s$  such that  $\Re z_i > 0$ . Then we have the following

**Proposition 1** *The Laplace transform of the function  $\text{map}_g(\xi)$  equals*

$$\int_{\mathbb{R}_{\geq 0}^s} e^{-(z,s)} \text{map}_g(\xi) \frac{d\xi}{\xi} = \frac{1}{2^{3g-3+3s/2-1}} \sum_{\Gamma \in \Gamma_{g,s}^3} \frac{1}{|\text{Aut}(\Gamma)|} \prod_{e \in e(\Gamma)} \frac{1}{\sqrt{z_{1,e}} + \sqrt{z_{2,e}}}. \quad (2.12)$$

Here  $\Gamma_{g,s}^3$  is the set of 3-valent ribbon graphs of genus  $g$  with  $s$  cells numbered by  $1, 2, \dots, s$ ,  $e(\Gamma)$  is the set of edges of  $\Gamma$ , and  $z_{1,e}$  and  $z_{2,e}$  are the two  $z_i$ 's which correspond to the two borders of an edge  $e \in e(\Gamma)$ .

The right-hand side is, up to the presence of square roots, identical to the right-hand side of the main formula in [18] as mentioned above in Section 1.6.

## 2.6

As an example, consider the case  $s = 1$ ,  $g = 1$ . In this case, the set  $\Gamma_{g,s}^3$  consists of one element which is displayed in Figures 6 and 7. The automorphism group of this graph is the cyclic group of order 6 which is clearly seen in the left half of Figure 6. Also, there is only one  $z$  which corresponds to both sides of every edge. Therefore,

$$\int_0^\infty e^{-z\xi} \text{map}_1(\xi) \frac{d\xi}{\xi} = \frac{1}{6} \frac{1}{2^{7/2}} \frac{1}{z^{3/2}},$$

which implies that

$$\text{map}_1(\xi) = \frac{1}{12\sqrt{\pi}} \left(\frac{\xi}{2}\right)^{3/2}.$$

In general, we have

$$\text{map}_g(\xi) \propto \xi^{3g-3/2}.$$

The constant can be fixed, for example, using the recurrence relations due to Harer and Don Zagier [14]

$$\begin{aligned} |\text{Map}_g(2k)| &= \frac{8k-2}{2k+1} |\text{Map}_g(2k-2)| + \\ &\quad \frac{(2k-1)(4k-1)(4k-3)}{2k+1} |\text{Map}_{g-1}(2k-4)|. \end{aligned}$$

It follows that

$$\text{map}_g(\xi) = \frac{1}{\sqrt{\pi}} \frac{1}{12^g g!} \left(\frac{\xi}{2}\right)^{3g-3/2}.$$

As an exercise, let us check that this is in agreement with the known density of the  $y_i$ 's (see e.g. [36]; remark that our  $y_i$ 's differ from the centered and scaled eigenvalues which are used in [36] by a factor of 2). The density of the  $y_i$ 's equals  $2K(2x)$  where

$$K(x) = \left(\frac{d}{dx} \text{Ai}(x)\right)^2 - x \text{Ai}(x)^2.$$

Here  $\text{Ai}(x)$  is the classical Airy function which is the unique, up to a constant factor bounded solution of the Airy equation  $f'' = xf$ .

Recall that the relation between  $\text{map}_g(\xi)$  and the density of the  $y_i$ 's is given by

$$2 \left\langle \sum_{i=1}^{\infty} \exp(\xi y_i) \right\rangle = \sum_{g \geq 0} \text{map}_g(\xi) = \frac{1}{\sqrt{\pi}} \left(\frac{\xi}{2}\right)^{-3/2} \exp\left(\frac{1}{12} \left(\frac{\xi}{2}\right)^3\right).$$

Therefore, we have to check the identity

$$\int_{-\infty}^{\infty} e^{\xi x} K(x) dx = \frac{1}{2\sqrt{\pi}} \frac{e^{\xi^3/12}}{\xi^{3/2}}. \quad (2.13)$$

One easily checks that

$$K''' - 4xK' + 2K = 0$$

therefore, its Laplace transform must satisfy a first order ODE which the right-hand side of (2.13) indeed satisfies. This yields the equality (2.13) up to a constant factor. The factor is fixed by the fact that

$$K(x) \sim \frac{\sqrt{-x}}{\pi}, \quad x \rightarrow -\infty$$

and that  $K(x)$  has a faster than exponential decay as  $x \rightarrow +\infty$ . Therefore its Laplace transform must grow like  $\frac{\xi^{-3/2}}{2\sqrt{\pi}}$  as  $\xi \rightarrow +0$ .

## 3 Random permutations

### 3.1

In the group algebra of the symmetric group  $S(n)$  consider the following elements  $X_1, X_2, \dots$

$$\begin{aligned} X_1 &= (12) + (13) + (14) + \dots, \\ X_2 &= (23) + (24) + (25) + \dots, \end{aligned}$$

and so on. These elements are called the Jucys-Murphy elements; for a modern introduction to their properties the reader is referred to [30]. These elements are truly remarkable in their simplicity: for example, they commute. In fact, they generate a maximal commutative subalgebra in the group algebra of  $S(n)$  which under Fourier transforms maps onto the algebra of operators diagonal in the Young basis. Since this fact is central to what follows, we shall review it briefly.

Let  $\lambda$  be a partition of  $n$  and consider the corresponding representation of the  $S(n)$ . Then the spectrum of the self-adjoint element  $X_1$  is labeled by the corners of the diagram  $\lambda$ . More precisely, if  $(i, \lambda_i)$  is a corner (that is, if  $\lambda_i > \lambda_{i+1}$ ) then  $\lambda_i - i$  is an eigenvalue of  $X_1$ . If one takes Figure 1 and adds the eigenvalues of the  $X_1$  one obtains Figure 12.

The  $(\lambda_i - i)$ -eigenspace of  $X_1$  is the irreducible representation of a smaller symmetric group corresponding to the diagram obtained from  $\lambda$  by deleting the square  $(i, \lambda_i)$ . We shall denote this diagram by  $\lambda^{[i]}$ . In particular, the multiplicity of the eigenvalue  $\lambda_i - i$  equals the dimension  $\dim \lambda^{[i]}$ .

Same argument now applies to  $X_2$  and the representation  $\lambda^{[i]}$ . It follows that the joint spectrum of the operators  $X_1$  and  $X_2$  in the representation  $\lambda$  is

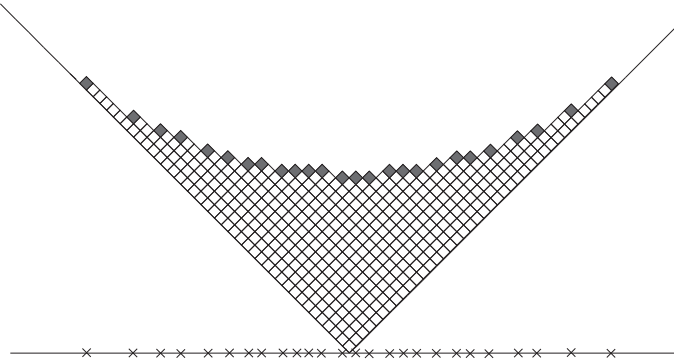


Figure 12: Eigenvalues of the  $X_1$

indexed by pairs of integers  $(i, j)$  such that  $\lambda^{[i]}$  and  $\lambda^{[i,j]}$  are both partitions (we abbreviate  $(\lambda^{[i]})^{[j]}$  to  $\lambda^{[i,j]}$ ). The corresponding eigenvalues are  $(\lambda_i - i, \lambda_j - j)$  if  $i \neq j$  and  $(\lambda_i - i, \lambda_i - i - 1)$  if  $i = j$ . The multiplicity of this pair of eigenvalues is  $\dim \lambda^{[i,j]}$ . Same considerations apply to any number of the  $X_i$ 's.

Observe that the ratio

$$\frac{\dim \lambda^{[i]}}{\dim \lambda}$$

is much simpler than the both then numerator and the denominator because most of the factors in any formula for the  $\dim \lambda$  cancel out. We shall be interested in the limit when  $i$  is fixed and  $\lambda$  is a Plancherel typical partition of  $n$ ,  $n \rightarrow \infty$ . One can show (using, for example, the main identity of [23] applied to the examples 5.2.7 and 7.2.9 of [23]) that in this limit

$$\frac{\dim \lambda^{[i_1, \dots, i_s]}}{\dim \lambda} \sim \frac{1}{n^{s/2}}.$$

Therefore, in the regular representation of  $S(n)$  we have

$$\frac{1}{2^{|k|} n^{(|k|-s)/2} n!} \text{tr} \prod_{i=1}^s X_i^{k_i} \sim \sum_{\lambda} \frac{(\dim \lambda)^2}{n!} \left( \sum_{i_1, \dots, i_s=1}^{\infty} \prod_{r=1}^s \left( \frac{\lambda_{i_r}}{2n^{1/2}} \right)^{k_r} + \dots \right), \quad (3.1)$$

where the dots stand for  $2^s - 1$  more sums of the form  $\sum_{i_1, \dots, i_s=1}^{\infty}$  which together with the lengths of the rows of the  $\lambda$  include the factors  $\left( -\frac{\lambda'_{i_r}}{2n^{1/2}} \right)^{k_r}$ ,

where  $\lambda'_i$  is the length of the  $i$ -th column of the diagram of  $\lambda$ . This is totally analogous to the fact that both the maximal and the minimal eigenvalues of a random matrix contribute to the asymptotics of (2.1).

In the above formula we assume that

$$k_i \sim n^{1/3} \xi_i, \quad n \rightarrow \infty$$

so that we can rely on  $(1 + n^{-1/2})^{n^{1/3}} \rightarrow 1$  as  $n \rightarrow \infty$ . By the same token, we conclude that

$$\frac{1}{n!} \operatorname{tr} \prod_{i=1}^s X_i^{k_i} \sim \frac{1}{n!} \operatorname{tr} \prod_{i=1}^s \tilde{X}_i^{k_i} \quad (3.2)$$

where the operators  $\tilde{X}_i$  are the following

$$\tilde{X}_i = (i, s+1) + (i, s+2) + \cdots + (i, n), \quad i = 1, \dots, s.$$

These operators no longer commute but they are more convenient for our purposes.

It is clear that the right-hand side of (3.2) equals the number of solutions  $\tau = (\tau_1, \dots, \tau_{|k|})$ ,  $\tau_i \in \{s+1, \dots, n\}$ , to the following equation in  $S(n)$

$$(1\tau_1) \cdots (1\tau_{k_1}) (2\tau_{k_1+1}) \cdots (2\tau_{k_1+k_2}) \cdots (s\tau_{|k|}) = 1. \quad (3.3)$$

The symmetric group  $S(n-s)$  acts naturally on the set of all solutions  $\{\tau\}$ . Let  $d(\tau)$  be the number of different numbers among the  $\tau_i$ 's. Then the  $S(n-s)$ -orbit of  $\tau$  consists of approximately  $n^{d(\tau)}$  elements. Indeed, since  $d(\tau) \leq |k| \propto n^{1/3}$  we have

$$\frac{n(n-1) \cdots (n-d(\tau))}{n^{d(\tau)}} \rightarrow 1, \quad n \rightarrow \infty.$$

It follows that

$$\frac{1}{n!} \operatorname{tr} \prod_{i=1}^s \tilde{X}_i^{k_i} \sim \sum_{\{\tau\}/S(n-s)} n^{d(\tau)}.$$

### 3.2

We now remark that the elements of the orbit set  $\{\tau\}/S(n-s)$  are in bijection with isomorphism classes of certain coverings of the sphere.

These corresponding coverings are defined as follows. Let  $0$  be the base point on the sphere and let  $|k|$  points be chosen on a circle around  $0$ . It is convenient to assume that  $|k| = 26$  and denote these points by letters of the English alphabet. Our covering will have simple ramifications over  $a, b, \dots, z$ . In the fiber over  $0$ , we pick  $s$  sheets and call them the *special* sheets. We further require the monodromy around each loop around  $a, b, \dots$  (see Figure 13 where a loop around  $b$  is shown) to be a transposition of a special sheet with a nonspecial one. Another requirement is that the first special sheet is

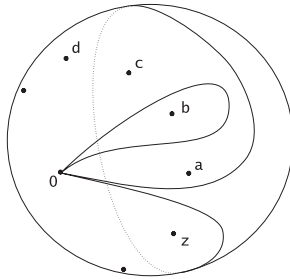


Figure 13: Paths of the monodromy

permuted by the first  $k_1$  loops, the second — by the next  $k_2$  loops and so on. (The product of all loops, which is the big loop in Figure 13, is contractible and so the product of the monodromies must be equal to 1.) Finally, we disallow any unramified sheets.

For fixed  $s, k_1, \dots, k_s$  there are only finitely many such coverings and we denote by  $\text{Cov}_S(k_1, \dots, k_s)$  those coverings which produce a fixed 2-manifold  $S$ .

It is clear, that once we choose any labeling of the non-special sheets in the fiber over  $0$  by the numbers  $\{s+1, \dots, n\}$  we get a solution of (3.3) and vice versa. We shall call the covering satisfying the above conditions the Jucys-Murphy coverings or *JM coverings* for short.

It is also clear that the covering corresponding to a  $\tau$  is  $(s + d(\tau))$ -fold covering with Euler number

$$\chi = 2d(\tau) + 2s - |k|.$$

Therefore, we conclude that

$$\frac{1}{2^{|k|} n^{(|k|-s)/2} n!} \text{tr} \prod_{i=1}^s X_i^{k_i} \sim \frac{1}{2^{|k|}} \sum_S n^{(\chi(S)-s)/2} |\text{Cov}_S(k_1, \dots, k_s)|. \quad (3.4)$$

Here the sum is over all homeomorphism types of orientable 2-manifolds without boundary, non necessarily connected. However, just as in (2.3) it is clear that it is sufficient to concentrate on connected surfaces only.

If  $S$  is a connected surface of genus  $g$  we shall denote the corresponding coverings by  $\text{Cov}_g(k_1, \dots, k_s)$ . It is clear that this set is empty unless  $|k|$  is even. In what follows, we shall always assume that  $|k|$  is even.

We shall prove the following

**Proposition 2** *As  $k_i \rightarrow \infty$ , we have*

$$\text{Cov}_g(k_1, \dots, k_s) \sim \text{Map}_g(k_1, \dots, k_s).$$

Since

$$\text{Map}_g(t \cdot \xi_1, \dots, t \cdot \xi_s) \sim 2^{t|\xi|} \text{map}_g(\xi) t^{3g-3+3s/2}$$

it follows that

$$\frac{|\text{Cov}_S(n^{1/3} \cdot \xi_1, \dots, n^{1/3} \cdot \xi_s)|}{2^{|n^{1/3}\xi|} n^{(s-\chi(S))/2}} \sim \frac{|\text{Map}_S(n^{2/3} \cdot \xi_1, \dots, n^{2/3} \cdot \xi_s)|}{2^{|n^{2/3}\xi|} n^{s-\chi(S)}}.$$

Comparing (2.3) with (3.4) establishes Theorem 1.

Note that the difference in the exponent of  $n$  in (2.3) and (3.4) is responsible for the difference in the scaling in (1.3) and (1.4).

The rest of this section is devoted to the proof of Proposition 2 and examples.

### 3.3

We shall now describe how to obtain a map on  $S$  from a JM covering  $S \rightarrow S^2$ . Let us make  $|k|$  cuts on the sphere from the points  $a, \dots, z$  to the infinity as in Figure 14. This cuts  $S$  into  $(s+d)$  polygons. Let us describe the shape of these polygons and how they fit together.

Given a nonspecial sheet  $\sigma$ , let its *valence* be the number of points from  $a, \dots, z$  such that the monodromy around that point permutes  $\sigma$ . Clearly, the valence of every sheet is  $\geq 2$ . On the other hand

$$\sum_{\text{nonspecial } \sigma} (\text{val}(\sigma) - 2) = |k| - 2d = 2s - \chi(S), \quad (3.5)$$

therefore the number of sheets of valence  $\geq 3$  is bounded by  $2s - \chi(S)$ .

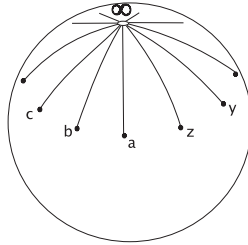


Figure 14: Cuts on the sphere

Suppose  $\sigma$  is a 2-valent sheet and suppose that the monodromy around one ramification point, say,  $p$  permutes it with the 1st special sheet and the monodromy around another ramification point, say,  $d$  permutes it with 2nd special sheet. Then the preimages of the cuts in Figure 14 on  $s$  are drawn in Figure 15 where the circled numbers 1 and 2 indicate that the corresponding boundary is attached to the 1st and 2nd special sheet, respectively. Note

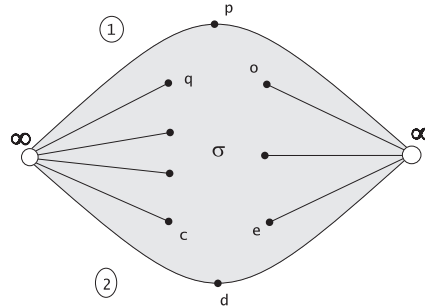


Figure 15: Nonspecial sheet of valence 2

how the angles get halved at the points which cover the points  $p$  and  $d$ .

Similarly, if  $\sigma$  is a 3-valent sheet then it looks like a triangle (similarly, a sheet of valence  $m$  looks like an  $m$ -gon). For example if monodromies around  $q$ ,  $c$ , and  $k$  permute  $\sigma$  with the 1st, 2nd, and 3rd special sheet, respectively, then  $\sigma$  looks like Figure 16.

The nonspecial sheets naturally glue together at the points which cover  $\infty$  to form a ribbon graph whose edges are the 2-valent sheets and vertices are either the sheets of valence  $\geq 3$  or multivalent junctions (like in Figure 26) of 2-valent sheets. See Figure 17 and note how  $q$  follows  $p$  and  $d$  follows  $c$  after passing through  $\infty$ .

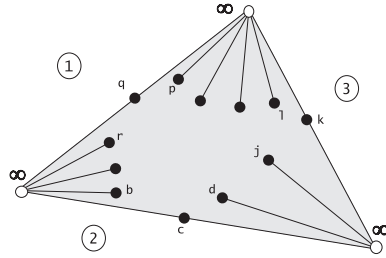


Figure 16: Nonspecial sheet of valence 3

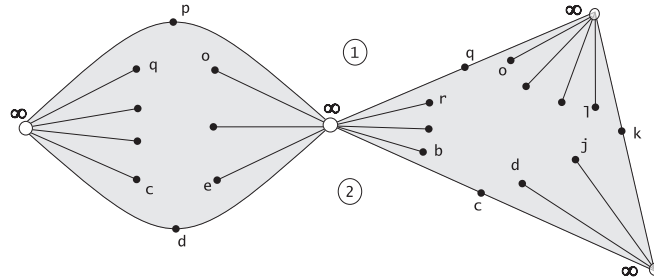


Figure 17: How nonspecial sheets fit together

Observe, in particular how we have the whole alphabet going once clockwise around each point over  $\infty$ . This reflects the fact that there is no ramification over  $\infty$ .

The cells of this ribbon graph correspond to the special sheets and look as follows. Suppose  $\sigma$  is the  $i$ -th special sheet. Then the valence of  $\sigma$  is, by construction, equal to  $k_i$ . Suppose that  $k_i = 6$  and the corresponding ramification points are  $\{l, m, m, o, p, q\}$ . Then this special sheet looks like the hexagon in Figure 18.

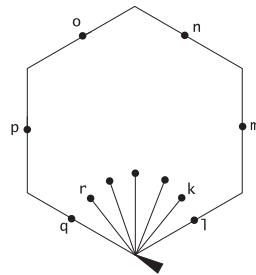


Figure 18: A special sheet with a marked vertex

As an example, consider the following solution to (3.3)

$$(12)(13)(12)(13)(12)(13) = 1,$$

which is the Coxeter relation in  $S(3)$ . The corresponding 3-fold covering of the sphere is a torus and the 3 sheets (one 6-valent special, two 3-valent nonspecial) fit together on the torus  $T^2$  shown in Figure 19.

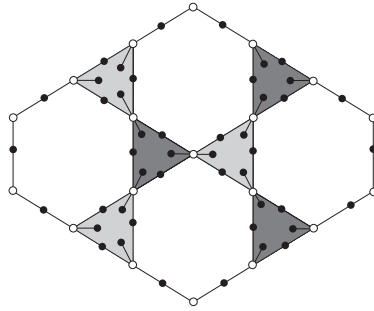


Figure 19: A 3-fold JM covering  $T^2 \rightarrow S^2$

### 3.4

We introduce now the following mapping  $\Psi$  from the set of JM coverings  $S \rightarrow S^2$  with  $s$  special sheets to the set of maps on  $S$  with  $s$  boundary components. We simply eliminate all nonspecial sheets as follows. If a nonspecial sheet  $\sigma$  is 2-valent then we plainly collapse it and glue together the two special sheets which  $\sigma$  separated. Nonspecial sheets of valence  $\geq 3$  we shrink to the middle as shown in Figure 20 where the collapse of the two nonspecial sheets from Figure 17 is shown (the meaning of the arrow in Figure 20 will be explained below). Note that collapsing a sheet  $\sigma$  of valence  $\text{val}(\sigma) \geq 3$  increases the length of each of the  $\text{val}(\sigma)$  boundaries involved by 1. For example, the boundary in Figure 20 is 3 units longer than the boundary in Figure 17.

Also, the special sheets come with a natural choice of the marked vertex; namely, the initial vertex of their first edge (in alphabetical order). Recall that the edges of the special sheets are labeled by the ramification points  $a, b, \dots, z$ . For example, in Figure 18 the bottom vertex becomes the marked vertex.

Observe that any map obtained from a JM covering has vertices of two following fundamentally different types. Introduce the following notion. Let

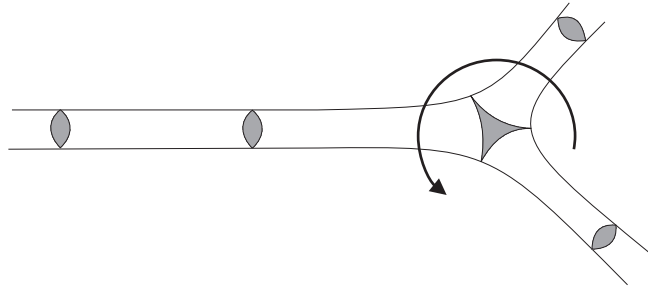


Figure 20: Collapse of Figure 17

$v$  be a vertex of a map. Suppose we are going around the boundary of the 1st polygon counterclockwise, then around the boundary of the 2nd polygon counterclockwise and so on. Then we visit our vertex  $\text{val}(v)$  times from the  $\text{val}(v)$  corners which meet at  $v$ . We call the vertex  $v$  a *right* vertex if the corners are visited in the clockwise order and a *left* vertex if the corners are visited in the counterclockwise order. By definition, we call  $v$  right if  $\text{val}(v) \leq 2$ .

Note that if  $\text{val}(v) > 3$  then  $v$  may be neither left nor right (for an example, look at the surface of genus 2 obtained by identifying opposite sides of a 10-gon). A left and right vertex of  $\text{val}(v) = 3$  are shown in Figure 21 where the dashed lines represent the order of going around the three corners.

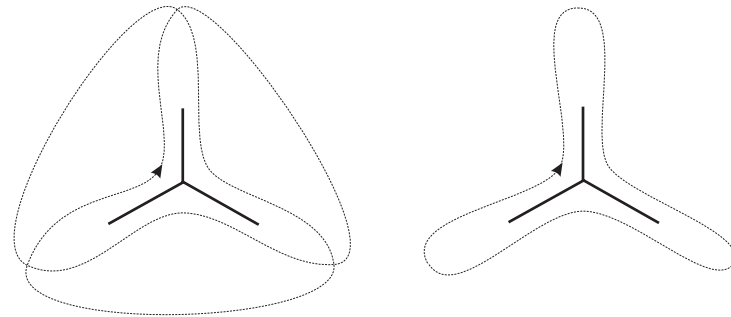


Figure 21: A left vertex and a right vertex

Now, suppose  $v$  is a vertex of map which came from of a JM covering. Then  $v$  either covers  $\infty$  or  $v$  is the middle point of a collapsed  $m$ -valent nonspecial sheet where  $m \geq 3$ . Observe that then  $v$  is a right or left vertex,

respectively. Indeed, if  $v$  covers  $\infty$  then, since there is no ramification over  $\infty$ , the whole alphabet is circling  $v$  once clockwise. Similarly, if  $v$  was a midpoint of a nonspecial sheet then (see Figure 16) the alphabet was going around  $v$  once counterclockwise. This translates into  $v$  being a right and left vertex, respectively.

For example, the arrow in Figure 20 shows the order of visiting the corners of the trivalent vertex (which is left).

### 3.5

We shall now prove the following:

**Lemma 1** *The mapping  $\Psi$  from JM coverings to maps is one-to-one. Its image  $\text{Im } \Psi$  consists of all maps satisfying the two following conditions:*

1. *every vertex is either left or right,*
2. *all marked vertices are interior right vertices.*

We call a vertex  $v$  an *interior* vertex if all corners which meet  $v$  come from the same polygon of the map. Recall that for vertices of valence  $> 4$  being left or right is a nontrivial condition and that was shown above that only left or right vertices arise from JM coverings.

*Proof.* By construction, all marked vertices come from some points which cover  $\infty$  and, therefore, they are right vertices. Let us show that they also must be interior vertices. This follows from inspection of Figure 22. The Figure 22 shows the marked vertex (the bottom one) of the special sheet from Figure 18.

Since the whole alphabet must go once around  $\infty$  the points marked by question marks in Figure 22 cannot be points from  $\{r, s, \dots, j, k\}$ . On the other hand, the points  $\{r, s, \dots, j, k\}$  are precisely the ramification points which *do not* lie on the boundary of our special sheet. Therefore, all points marked by question marks do lie on the boundary of our special sheet. It follows that all corners in Figure 22 come from one and the same special sheet.<sup>3</sup>

---

<sup>3</sup>The condition that the initial vertex must be an interior vertex can also be understood as follows. Let  $\tau$  be a solution of (3.3). Then  $(1\tau_1) \cdots (1\tau_{k_1})$  must fix 1 because 1 is clearly fixed by the rest of the product in (3.3). This translates into Figure 22.

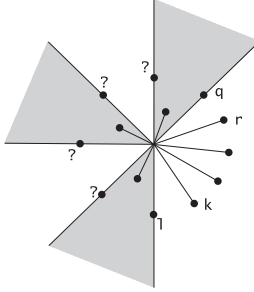


Figure 22: The marked vertex must be an inner vertex

We shall now show that any map satisfying the above two conditions come from a unique JM covering. This covering can be reconstructed as follows.

Assign symbols  $a, b, c, \dots$  consecutively to all edges of the polygons of the map starting from the marked vertex of the first polygon.

Now consider some vertex  $v$  of our map. If  $v$  is a right vertex (in particular, if  $\text{val}(v) \leq 2$ ) then the structure of the corresponding JM covering at  $v$  can be reconstructed uniquely from the fact that  $v$  covers  $\infty$  and there is no ramification at  $\infty$ . (In other words, all letters of the alphabet have to occur once clockwise around  $v$ ).

This reconstruction is shown, respectively, in Figures 23 for the case  $\text{val}(v) = 1$ , in Figure 24 for the case  $\text{val}(v) = 2$ , and in Figures 25 and 26 for  $\text{val}(v) = 3$ .

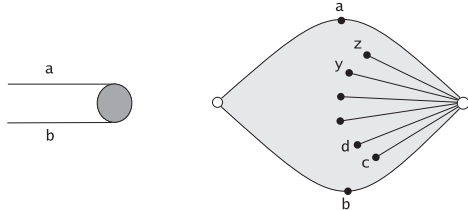


Figure 23: Reconstruction of JM covering for  $\text{val}(v) = 1$

When we encounter a left vertex (such as the vertex with the arrow in Figure 20) then we insert a nonspecial sheet of valence  $\text{val}(v)$ . (The result looks like Figure 16). A small detail is that this operation reduces the number of edges by  $\text{val}(v)$  and we have to relabel the edges if we want a consecutive alphabetical labeling.

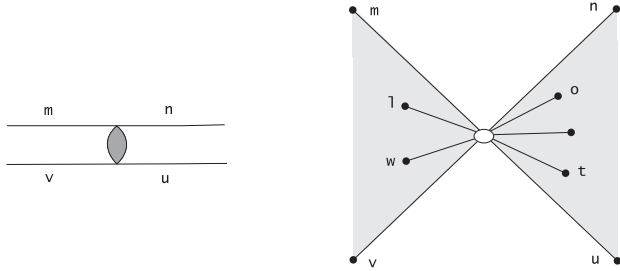


Figure 24: Reconstruction of JM covering for  $\text{val}(v) = 2$

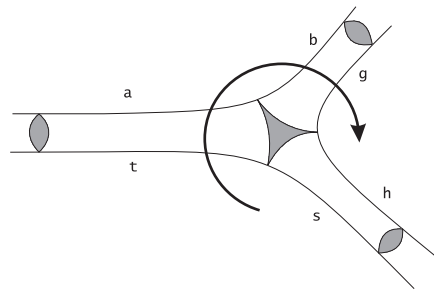


Figure 25: A right vertex of valence 3

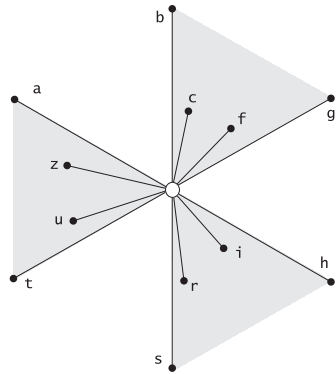


Figure 26: The JM covering corresponding to a right vertex of valence 3

Finally, if the edges of a polygon of a map are labeled by  $l, m, \dots, p, q$  and its initial vertex is an interior right vertex then there is always room to fit the rest of the alphabet as in Figure 22. This concludes the proof of Lemma 1.

### 3.6

In this subsection we shall use the abbreviation

$$k = (k_1, \dots, k_s).$$

Denote by  $\text{Map}_g^3(k)$  the set of maps such that, after elimination of vertices of valence  $\leq 2$ , they have only trivalent vertices. Since only trivalent vertices contribute to (2.11), we know that

$$|\text{Map}_g^3(k)| \sim |\text{Map}_g(k)|, \quad k_i \rightarrow \infty. \quad (3.6)$$

Similarly, denote by  $\text{Map}_g^*(k)$  the subset of  $\text{Map}_g^3$  formed by maps such that all their vertices are either right or trivalent and the marked vertex of each polygon is an interior right vertex. It follows from Lemma 1 that  $\text{Map}_g^* \subset \text{Im } \Psi$ , and, moreover, it is in the image of JM coverings with nonspecial sheets of valence  $\leq 3$ .

We shall now establish the following

**Lemma 2** *We have*

$$|\text{Map}_g^*(k)| \sim 2^{-6g+6-6s} |\text{Map}_g^3(k)| \quad (3.7)$$

$$|\text{Im } \Psi \cap \text{Map}_g^3 \setminus \text{Map}_g^*| = o(|\text{Map}_g^*|). \quad (3.8)$$

Once Lemma 2 is established, the Proposition 2 will follow. Indeed, since  $\Psi$  is one-to-one, then because of (3.6) and (3.8) it suffices to consider coverings with only  $\leq 3$ -valent nonspecial sheets. For such a covering, the number of 3-valent sheets equals  $2g - 2 + 2s$ . Collapsing a trivalent sheet to its middle increases the length of the boundary by 3. Therefore, in total, the boundary of the corresponding map is  $6g - 6 + 6s$  longer. Since this precisely compensates the exponent in (3.7), we obtain:

$$|\text{Cov}_g(k)| \sim |\text{Map}_g(k)|, \quad k \rightarrow \infty.$$

We shall now proceed with the proof of Lemma 2. First, in order to examine the difference between the sets  $\text{Map}_g^3$ ,  $\text{Map}_g^*$ , and  $\text{Im } \Psi$  we need to introduce the following notions.

Let  $v_0$  be a marked vertex of a map with  $s > 1$  polygons. Suppose that  $v_0$  is an interior vertex. Follow the edges of the corresponding polygon in the counterclockwise direction until we reach a vertex  $v$  which is not interior.

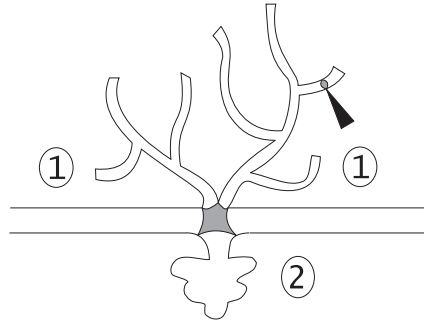


Figure 27: A mouth vertex

By analogy with the flow of a river, we call the vertex  $v$  a *mouth* vertex, see Figure 27. Observe that a mouth vertex is *never right*.

Also, call a vertex  $v$  of a map *contractible* if it disappears after contraction of all  $\leq 2$ -valent vertices; otherwise, call it *incontractible*. Observe that a contractible vertex is always right unless it is a mouth vertex.

*Proof.* First, the condition that the marked vertices must be right is asymptotically negligible. Indeed, all but finitely many vertices are right and the chances to hit one them with a mark go to 1 as the perimeter goes to infinity.

The possible combinatorial configurations of the incontractible and mouth vertices of maps in  $\text{Map}_g^3$  are described by ribbon graphs  $\Gamma \in \Gamma_g^3$  together with the choice of an edge  $e_i \in e(\Gamma)$ ,  $i = 1, \dots, s$ , on the boundary of any cell of  $\Gamma$ . The edge  $e_i$  is the first edge we reach if we start from the marked vertex of the  $i$ -th cell of the map. We shall see that, for any configuration, the proportion of maps lying in  $\text{Map}_g^*$  equals  $\sim 2^{-6g+6-6s}$ , and that the same portion of maps lies in  $\text{Im } \Psi$ . This number is, in fact, a product of factors  $2^{-3}$  over the  $2g - 2 + s$  vertices  $v$  that are not right. Let us examine such vertices  $v$ .

First, suppose  $v$  is an incontractible vertex. By definition of  $\text{Map}_g^3$ , it means that  $v$  becomes trivalent after the 3 forests shown in Figure 28 are contracted onto it. We claim that for such a vertex being left is equivalent to being trivalent. Indeed, suppose  $v$  is left and not trivalent. Then, as we go around any nonempty tree in any of the forests shown in Figure 28, we go from one corner of  $v$  to the next corner in the clockwise direction. Since  $v$  is left, this is impossible.

It follows from the discussion in Section 2.4 that the removal of any given forest comes at the price of the factor  $\frac{1}{2}$  in the asymptotics. Therefore,

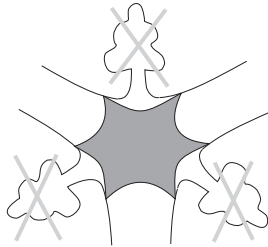


Figure 28: The forbidden forests of a left vertex

asymptotically  $\sim \frac{1}{2^3}$  of maps are trivalent at  $v$  or, equivalently,  $v$  is a left (or trivalent) vertex for about  $\sim \frac{1}{2^3}$  of all maps.

Now suppose that  $v$  is a contractible mouth vertex, such as the one shown in Figure 27. We may assume that  $v$  does not coincide with any other mouth vertex because the chances of such a coincidence vanish as the perimeter of the map goes to infinity.

With this assumption,  $v$  being left is again equivalent to  $v$  being trivalent and both mean that  $v$  must look like the vertex in Figure 29: namely, the

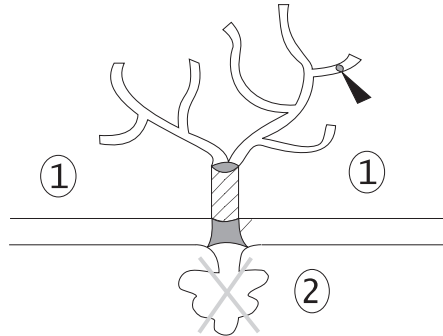


Figure 29: A trivalent contractible mouth vertex

forest at the bottom must be empty and only one branch (shaded in Figure 29) must go up.

For general maps, multiple branches may go up or no branches at all (which means that the marked vertex is not interior). Therefore, the insertion of this shaded branch and chopping down the forest at the bottom takes arbitrary maps to maps such that  $v$  is a trivalent mouth vertex and the corresponding marked vertex is interior. The insertion of the shaded branch increases the perimeter by 2. This means that  $\sim \frac{1}{2^2}$  of maps have it. This

times  $\sim \frac{1}{2}$  for the forest gives us the total of  $\sim \frac{1}{2^3}$  of maps belonging to  $\text{Map}_g^*$  or, equivalently, to  $\text{Im } \Psi$ .

Either way, we get a factor of  $2^{-3}$  for any trivalent left vertex. The number of such vertices can be easily computed. All of them become trivalent nonspecial sheets of the corresponding JM covering. Therefore, by (3.5) there are  $2g - 2 + 2s$  of them. This proves (3.7) and (3.8) and concludes the proof of Lemma 2, Proposition 2, and Theorem 1.

### 3.7

As an example, consider the cases  $s = 1$  and  $g = 0, 1$ . If  $g = 0$  then there are no nonspecial sheets of valence  $> 2$  and, hence, the sets  $\text{Cov}_0(k)$  and  $\text{Map}_0(k)$  are in bijection. Simply put, this means that if among the numbers  $i_1, \dots, i_k$  there are precisely  $k/2$  pairs of equal numbers then

$$(1i_1)(1i_2) \dots (1i_k) = 1 \quad (3.9)$$

if and only if the corresponding pairing is noncrossing as in example in Section 2.2. This observation is due to P. Biane.

Note that the noncrossing in (3.9) means that this equality is a consequence of solely the relations

$$(1i)^2 = 1, \quad i = 1, 2, \dots,$$

among the generators (12), (13), (14),  $\dots$  of the symmetric group. The relations of Coxeter type (which produce coverings of genus 1)

$$(1i)(1j)(1i)(1j)(1i)(1j) = 1$$

start playing role in the enumeration of  $\text{Cov}_1(k)$ .

Every covering in  $\text{Cov}_1(k)$  has either two 3-valent special sheets or, else, one of valence 4. Consider the first case because the second makes no contribution to the asymptotics. Denote by  $\text{Cov}_1^3(k)$  the corresponding subset of  $\text{Cov}_1(k)$ .

For  $\text{Cov}_1^3(k)$ , the corresponding relations are, up to a cyclic shift:

$$(1i) w_1 (1j) w_2 (1i) w_3 (1j) w_4 (1i) w_5 (1j) w_6 = 1 \quad (3.10)$$

Here the  $w_i$ 's are some words in the generators (12), (13), (14),  $\dots$  subject to two conditions. First,  $(1i)$  and  $(1j)$  appear exactly 3 times each in (3.10) and any other generator appears either 0 or 2 times. Second,

$$w_1 w_4 = w_2 w_5 = w_3 w_6 = 1,$$

which means that any relation (3.10) is built from 3 relations from the  $g = 0$  case. Using the generating function (2.6) for the number of the noncrossing pairings, one obtains the following generating functions.

$$\sum_k |\text{Cov}_1^3(k)| z^k = \frac{1}{4} \frac{z^2 (1 - \sqrt{1 - 4z^2})^2}{(1 - 4z^2)^{5/2}}.$$

Since

$$\frac{1}{4} \frac{z^2 (1 - \sqrt{1 - 4z^2})^2}{(1 - 4z^2)^{5/2}} \sim \frac{1}{16} \frac{1}{(1 - 4z^2)^{5/2}}, \quad z^2 \rightarrow \frac{1}{4},$$

we conclude that

$$\frac{|\text{Cov}_1(k)|}{2^k} \sim \frac{|\text{Cov}_1^3(k)|}{2^k} \sim \frac{1}{16} \frac{(k/2)^{\frac{5}{2}-1}}{\Gamma(5/2)} = \frac{1}{12\sqrt{\pi}} \left(\frac{k}{2}\right)^{3/2},$$

which agrees with computations of Section 2.6

## References

- [1] D. Aldous and P. Diaconis, *Hammersley's interacting particle process and longest increasing subsequences*, Prob. Theory and Rel. Fields, **103**, 1995, 199–213.
- [2] J. Baik, P. Deift, K. Johansson, *On the distribution of the length of the longest increasing subsequence of random permutations*, math.CO/9810105.
- [3] J. Baik, P. Deift, K. Johansson, *On the distribution of the length of the second row of a Young diagram under Plancherel measure*, math.CO/9901118.
- [4] P. Biane, *Permutation model for semi-circular systems and quantum random walks*, Pacific J. Math., **171**, no. 2, 1995, 373–387.
- [5] P. Biane, *Representations of symmetric groups and free probability*, Adv. Math., **138**, 1998, no. 1, 126–181.
- [6] S. Bloch and A. Okounkov, *The character of the infinite wedge representation*, alg-geom/9712009.

- [7] A. Borodin and G. Olshanski, *Distribution on partitions, point processes, and the hypergeometric kernel*, math.RT/9904010.
- [8] A. Borodin, A. Okounkov, and G. Olshanski, *On asymptotics of the Plancherel measures for symmetric groups*, math.CO/9905032.
- [9] P. Diaconis and C. Greene, *Applications of Murphy's elements*, Stanford University Technical Report, no. 335, 1989.
- [10] R. Dijkgraaf, *Mirror symmetry and elliptic curves*, The Moduli Space of Curves, R. Dijkgraaf, C. Faber, G. van der Geer (editors), Progress in Mathematics, **129**, Birkhäuser, 1995.
- [11] A. Eskin and A. Okounkov, in preparation.
- [12] P. J. Forrester, *The spectrum edge of random matrix ensembles*, Nuclear Phys. B, **402**, 1993, no. 3, 709–728.
- [13] P. Di Francesco, P. Ginsparg, J. Zinn-Justin, *2D gravity and random matrices*, Phys. Rep. **254**, 1995, 1–133.
- [14] J. Harer and D. Zagier, *The Euler characteristic of the moduli space of curves*, Invent. Math., **85**, 1986, 457–485.
- [15] K. Johansson, *The longest increasing subsequence in a random permutation and a unitary random matrix model*, Math. Res. Letters, **5**, 1998, 63–82.
- [16] K. Johansson, *Discrete orthogonal polynomial ensembles and the Plancherel measure*, math.CO/9906120.
- [17] A. Jucys, *Symmetric polynomials and the center of the symmetric group ring*, Reports Math. Phys., **5**, 1974, 107–112.
- [18] M. Kontsevich, *Intersection theory on the moduli space of curves and the matrix Airy function*, Commun. Math. Phys., **147**, 1992, 1–23.
- [19] S. Kerov, *Gaussian limit for the Plancherel measure of the symmetric group*, C. R. Acad. Sci. Paris, **316**, Série I, 1993, 303–308.
- [20] S. Kerov, *Transition probabilities of continual Young diagrams and the Markov moment problem*, Func. Anal. Appl., **27**, 1993, 104–117.

- [21] S. Kerov, *The asymptotics of interlacing roots of orthogonal polynomials*, St. Petersburg Math. J., **5**, 1994, 925–941.
- [22] S. Kerov, *A differential model of growth of Young diagrams*, Proceedings of the St. Petersburg Math. Soc., **4**, 1996, 167–194.
- [23] S. Kerov, *Interlacing measures*, Amer. Math. Soc. Transl., **181**, Series 2, 1998, 35–83.
- [24] S. Kerov and A. Okounkov, *A new proof of Thoma theorem*, unpublished paper, 1995.
- [25] A. Klyachko and E. Kurtaran, *Some identities and asymptotics for characters of the symmetric group*, J. Algebra, **206**, no. 2, 1998, 413–437.
- [26] G. Murphy, *A new construction of Young's seminormal representation of the symmetric group*, J. Algebra, **69**, 1981, 287–291.
- [27] A. Okounkov, *On the representations of the infinite symmetric group*, Zapiski Nauchnyh Seminarov POMI, **240**, 1997, 167–230, available from math/9803037.
- [28] A. Okounkov, *Wick formula, Young basis, and higher Capelli identities*, Internat. Math. Res. Notices, 1996, no. 17, 817–839.
- [29] A. Okounkov, *Infinite wedge and measures on partitions*, math.RT/9907127.
- [30] A. Okounkov and A. Vershik, *A new approach to representation theory of symmetric groups*, Selecta Math. (N.S.), **2**, 1996, no. 4, 581–605.
- [31] B. F. Logan and L. A. Shepp, *A variational problem for random Young tableaux*, Adv. Math., **26**, 1977, 206–222.
- [32] E. M. Rains, *Increasing subsequences and the classical groups*, Electr. J. of Combinatorics, **5**(1), 1998.
- [33] T. Seppäläinen, *A microscopic model for Burgers equation and longest increasing subsequences*, Electron. J. Prob., **1**, no. 5, 1996.
- [34] Ya. Sinai and A. Soshnikov, *A refinement of Wigner's semicircle law in a neighborhood of the spectrum edge for random symmetric matrices*, Func. Anal. Appl., **32**, 1998, no. 2, 114–131.

- [35] A. Soshnikov, *Universality at the edge of the spectrum in Wigner random matrices*, math-ph/9907013.
- [36] C. A. Tracy and H. Widom, *Level-spacing distributions and the Airy kernel*, Commun. Math. Phys., **159**, 1994, 151–174.
- [37] A. Vershik and S. Kerov, *Asymptotics of the Plancherel measure of the symmetric group and the limit form of Young tableaux*, Soviet Math. Dokl., **18**, 1977, 527–531.
- [38] A. Vershik and S. Kerov, *Asymptotics of the maximal and typical dimension of irreducible representations of symmetric group*, Func. Anal. Appl., **19**, 1985, no.1.
- [39] A. Zvonkin, *Matrix integrals and map enumeration: an accessible introduction*, Math. Comput. Modelling, **26**, 1997, no. 8–10, 281–304.

*E-mail address:* okounkov@math.berkeley.edu